Characterization of oxide precipitates in epitaxial InN by transmission electron microscopy

X. Xu, P. Specht, R. Armitage, J. C. Ho, and E. R. Weber
Department of Materials Science and Engineering, University of California, Berkeley and Materials Science Division, Lawrence Berkeley National Laboratory, Berkeley, California 94720

C. Kisielowski
National Center for Electron Microscopy, Lawrence Berkeley National Laboratory, Berkeley, California 94720

(Received 17 May 2005; accepted 18 July 2005; published online 23 August 2005)

InN thin films have been grown epitaxially on GaN-buffered sapphire substrates by molecular-beam epitaxy at 500 °C. A high level of oxygen contamination in the growth chamber led to formation of In_2O_3 precipitates in the films. These precipitates were characterized in detail by transmission electron microscopy (TEM). The concentration of In_2O_3 was estimated to be less than 0.07 vol % in the present samples of oxygen content ~0.5 at. %. Cross-sectional TEM investigations revealed that the precipitates adopt a preferred crystallographic orientation within the InN matrix, and show a characteristic diameter of ~5 nm with average distance of ~500 nm. These observations suggest the effective solubility of O in InN could be below 1 at. % at 500 °C. © *2005 American Institute of Physics*. [DOI: 10.1063/1.2035330]

InN finds applications in the form of InGaN alloys which are now widely used in commercial optoelectronics in the green-to-ultraviolet spectral region. InN is also considered an interesting material for future applications in high mobility transistors and near-infrared optoelectronics. However, some important fundamental properties of InN are still not well understood. Unintentionally doped InN samples can exhibit very high free electron concentrations up to the mid-10^{20} cm^{-3}, the origin of which has not been explained. Additionally, widely varying values of the band gap energy of InN (0.6–2.2 eV) are reported in the literature, and the origin of these variations is the subject of much debate.[1–6]

The role of oxygen in InN is an interesting topic given the unresolved issues discussed above. O_N has been proposed as a likely candidate for the major residual donor species in InN.[7] Oxygen alloying has been suggested as a possible cause of variations in the band gap of InN,[8–10] although this idea seems implausible even for oxygen concentrations exceeding 10 at. % unless the $InN_{1-x}O_x$ system exhibits a very large bowing parameter.[11] In any case, before proposing theories based on alloying effects one should consider the basic question of oxygen solubility in InN. To our knowledge, there is no direct evidence that *alloys* (as opposed to *mixtures*) of appreciable oxygen concentration form in InN. In the present work we show that precipitation of In_2O_3 occurs in layers of oxygen concentration ~0.5 at. %, as measured by secondary ion mass spectrometry (SIMS). Both high resolution electron microscopy (HREM) technique and electron energy loss spectroscopy (EELS) techniques were used to analyze two epitaxial InN samples grown by MBE on GaN-buffered *c*-plane sapphire substrates. The crystallographic orientation relationship of the In_2O_3 precipitates and InN matrix was revealed, and the concentration of In_2O_3 was estimated and related to the total oxygen concentration in the samples measured by SIMS.

Two InN samples were investigated, Nos. 903 and 904. The GaN buffer layer for No. 903 was grown by MBE with a thickness of 30 nm, and the GaN buffer layer for No. 904 was grown by metalorganic chemical vapor deposition (MOCVD) with a thickness of 2 μm. The InN film thickness for both samples is about 1 μm. Details of the growth procedure have been described previously.[12] Due to an air leak in the MBE chamber, an oxygen partial pressure estimated to be in the 10^{-8} Torr range was present during InN growth. After growth, the samples were annealed in a tube furnace with flowing N_2 gas at 600 °C for 4 h. Before annealing, an amorphous AlN film of thickness ~100 nm was deposited on the InN surface by rf sputtering at room temperature to prevent the InN surface from decomposing and prevent oxidation. SIMS measurements have shown that the oxygen concentration in the samples is of the order of $10^{20}/cm^3$.[12]

TEM specimens were prepared in cross section geometry with both [01-10] and [2-1-10] orientations, and thinned to electron transparency by Ar ion milling with voltage 5 keV, low angle (8°). During ion milling, liquid nitrogen cooling was used to protect the samples from overheating. The samples were then subjected to lower voltage (2 keV) ion milling to remove surface damage.

HREM images of No. 904 showed that both hexagonal and cubic InN phases coexist in the InN layer. Figure 1(a) shows an image taken with the Philips CM300 microscope. A fast Fourier transform (FFT) pattern [Fig. 1(b)] from the

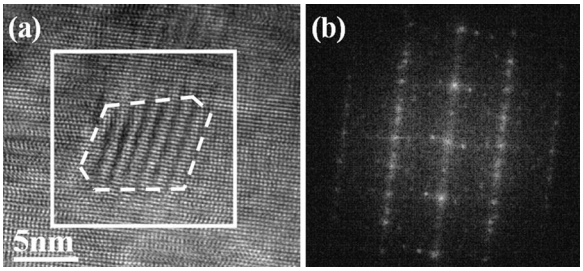

FIG. 1. (a) HREM image projected from InN $[2\bar{1}\bar{1}0]$ orientation showing a precipitate in sample No. 904; (b) the FFT pattern of the marked area in image (a).

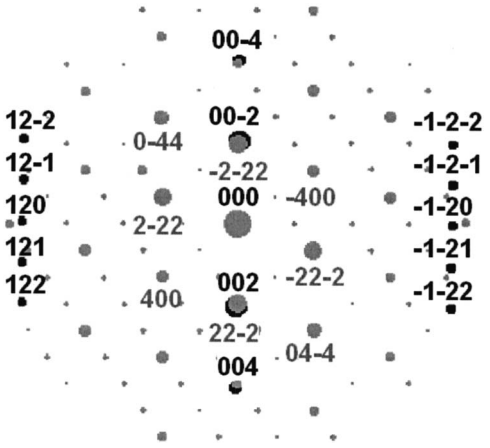

FIG. 2. Diffraction pattern simulated from hexagonal InN and In_2O_3 layered structure. Projected orientation is [011] for In_2O_3 and $[2\bar{1}\bar{1}0]$ for InN.

marked square region in Fig. 1(a) was extracted using the software *Digital Micrograph*. The coincidence of the spot indexed (-11-1) in the cubic phase and the spot indexed (0002) in the hexagonal phase indicates that the spacing between {111} planes in the cubic phase nearly equals the spacing between {0002} planes in the hexagonal phase. The orientation relationship between the two InN phases is [011]// [2-1-10] and [-11-1]//[0002]. Precipitates were found in this sample, as seen both from the Moiré fringe in Fig. 1(a) and from the presence of a third set of diffraction spots (in addition to the spots from the hexagonal and cubic InN phases) in Fig. 1(b). To identify the precipitate, we simulated an overlaid structure of wurtzite InN and In_2O_3 (Fig. 2) with the software MACTEMPAS. Since the corresponding angles and distances between the spots in both the simulation and the experiment are comparable, the precipitate found in Fig. 1 was determined as In_2O_3. In_2O_3 has the MnO_2-type structure, and there are 80 atoms per unit cell, 32 indium atoms and 48 oxygen atoms. The lattice parameter used in the simulation was 10.117 Å.[13] X-ray diffraction measurements showed that the wurtzite InN grains in the sample have the lattice parameters a=3.535 Å, c=5.799 Å.[12] The projected orientation of the InN matrix is [2-1-10], and that of the In_2O_3 precipitate is [011]. The coincidence between the diffraction spot (000-2) in InN and (-2-22) in In_2O_3 indicates that the In_2O_3 (111) planes are parallel to the InN (0001) planes. An atomic model created using the software CRYSTALKIT, in which the lattice parameters, space groups, and orientation

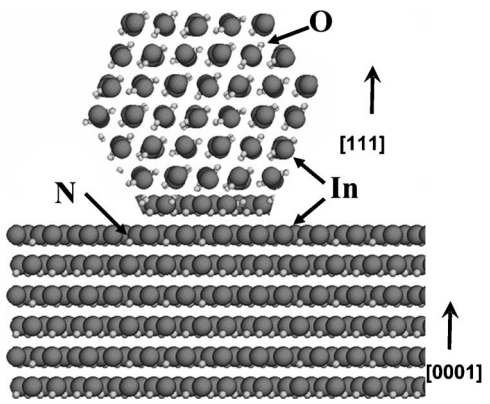

FIG. 3. An atomic model created using the software CRYSTALKIT illustrates the orientation relationship between an In_2O_3 precipitate and hexagonal InN.

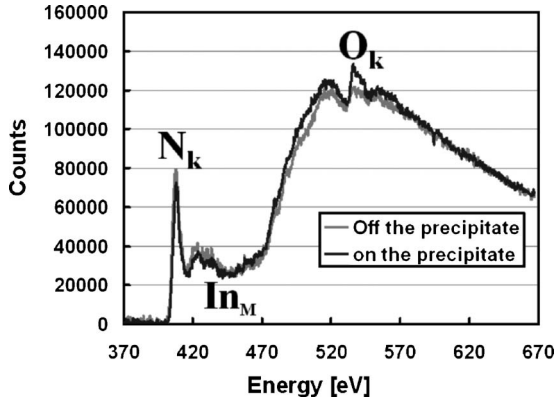

FIG. 4. EELS spectra collected from the precipitate in the Fig. 1(a) and InN matrix, respectively.

relationship between two structures are defined, illustrates the geometry of the In_2O_3 precipitate and InN matrix as shown in Fig. 3.

EELS analysis on the precipitate (shown in Fig. 4) was performed at the same time the image was acquired. The EELS has a spot size of 10 nm and energy resolution 1 eV. One curve shows data obtained from the precipitate, and another curve data obtained from the matrix (at a position close to the precipitate so as to minimize the thickness effect). Sample drift was checked before and after collecting the spectrum, and was less than 1 nm. As seen from the plot, nitrogen K-edge is at 401 eV, and the indium $M_{4,5}$ edges is at 451 eV. Both the indium and oxygen counts are higher, and the nitrogen counts are lower, on the particle than that off the particle. This provides further evidence that the particle is In_2O_3 (perfect correlation of the EELS signals to InN and In_2O_3 is not expected, since the measured volume is larger than the precipitate). We can exclude the possibility that In_2O_3 precipitates were introduced during mechanical preparation of the TEM specimen, since sample No. 904 was etched prior to TEM observation to remove any possible surface contamination related to sample processing, and in InN TEM samples which were prepared similarly but with lower overall oxygen contamination no precipitates were found.

In_2O_3 precipitates were also observed in sample No. 903, following the same TEM analysis procedure. Sample No. 903 did not contain a detectable volume of cubic InN. One of the precipitates in sample No. 903 is shown in Fig. 5, and the inset shows the corresponding FFT pattern. The estimated percentage of In_2O_3 is 0.07 vol % or less, which is

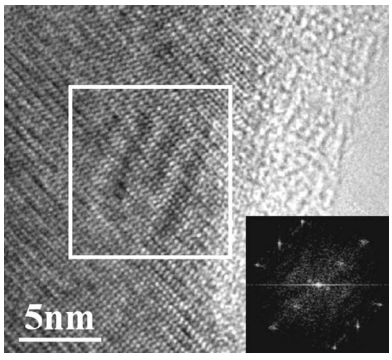

FIG. 5. High resolution transmission electron microscopy image projected from $[2\bar{1}\bar{1}0]$ orientation showing In_2O_3 precipitate in sample No. 903, inset shows FFT pattern of the marked area in the image.

calculated from the area of In_2O_3 over the total observed area of the sample, assuming uniform thickness. The average distance between the precipitates is estimated to 500 nm. The size of the In_2O_3 precipitates is around 5 nm, and they all have the same preferred orientation within the InN matrix as was observed in sample No. 904. For the present InN processing conditions, this appears to be an energetically favorable size and orientation of In_2O_3 precipitates.

Although different growth techniques were used to prepare the GaN buffer layers, both InN films contain In_2O_3 precipitates. It cannot be established for certain if the precipitates formed during the MBE growth or post-growth annealing. However the transport properties of the layers from Hall effect measurements did not change after annealing, suggesting the precipitates may have been already present in the as-grown layers. This suggests the effective solubility of O in InN is below 1 at. % at 500 °C. The volume fraction of In_2O_3 precipitates in the present samples is much too low to significantly affect their optical absorption and reflection spectra, although other material properties, e.g., electron mobility, might be affected by the concentration reduction of ionized impurities. An important consequence of In_2O_3 precipitation is that the concentration of O_N donors in heavily doped InN samples may be significantly less than the oxygen concentration measured by SIMS. Calculation shows there could be up to 50 at. % O formed precipitates from the InN matrix.

In summary, In_2O_3 precipitates were identified by HREM and EELS analysis in oxygen-contaminated InN epilayers grown by MBE ([O] ~0.5 at. %) using two types of GaN buffer layers on *c*-plane sapphire. The In_2O_3 volume concentration is estimated as less than 0.07 vol % in the present samples. The characteristic size of the precipitates is ~5 nm. Comparison with simulation results indicates that the preferred orientation of In_2O_3 relative to the InN matrix is [011]//[2-1-10] and [111]//[0001]. Additionally, the measured size and orientation of the precipitates can serve as input parameters for theoretical calculations of properties such as the InN/In_2O_3 interfacial energy.

This work was financially supported by the Air Force Office of Scientific Research under Contract No. FA9550-04-1-0408 (Program Manager J. Witt) and by the Director, Office of Science, Office of Basic Energy Sciences, Division of Materials Sciences, of the U.S. Department of Energy under Contract No. DE-AC03-76SF00098. The usage of the National Center for Electron Microscopy, LBNL, is greatly appreciated.

[1] K. S. A. Butcher, J. Cryst. Growth **269**, vii (2004).
[2] T. L. Tansley and C. P. Foley, J. Appl. Phys. **59**, 3241 (1986).
[3] J. Wu, W. Walukiewicz, K. M. Yu, J. W. Ager, E. E. Haller, H. Lu, W. J. Schaff, Y. Saito, and Y. Nanishi, Appl. Phys. Lett. **80**, 3967 (2002).
[4] T. V. Shubina, S. V. Ivanov, V. N. Jmerik, D. D. Solnyshkov, V. A. Vekshin, P. S. Kop'ev, A. Vasson, J. Leymarie, A. Kavokin, H. Amano, K. Shimono, A. Kasic, and B. Monemar, Phys. Rev. Lett. **92**, 117407 (2004).
[5] V. Y. Davydov, A. A. Klochikhin, R. P. Seisyan, V. V. Emtsev, S. V. Ivanov, F. Bechstedt, J. Furthmuller, H. Harima, V. Mudryi, J. Aderhold, O. Semchinova, and J. Graul, Phys. Status Solidi B **229**, R1 (2002).
[6] P. Specht, J. C. Ho, X. Xu, R. Armitage, E. R. Weber, R. Erni, and C. Kisielowski, Solid State Commun. **135**, 340 (2005).
[7] C. Stampfl, C. G. Van de Walle, D. Vogel, P. Kruger, and J. Pollmann, Phys. Rev. B **61**, R7846 (2000).
[8] A. G. Bhuiyan, K. Sugita, K. Kasashima, A. Hashimoto, A. Yamamoto, and V. Y. Davydov, Appl. Phys. Lett. **83**, 4788 (2003).
[9] M. Yoshimoto, H. Yamamoto, W. Huang, H. Harima, J. Saraie, A. Chayahara, and Y. Horino, Appl. Phys. Lett. **83**, 3480 (2003).
[10] D. Alexandrov, K. Scott, A. Butcher, and M. Wintrebert-Fouquet, J. Vac. Sci. Technol. A **22**, 954 (2004).
[11] T. L. Tansley, Presentation at the First International Indium Nitride Workshop, Fremantle, Australia, 16–20 November 2003.
[12] P. Specht, R. Armitage, J. Ho, E. Gunawan, Q. Yang, X. Xu, C. Kisielowski, and E. R. Weber, J. Cryst. Growth **269**, 111 (2004).
[13] W. B. Pearson, *Pearson's Handbook of Crystallographic Data for Intermetallic Phases*, 2nd ed. (American Society for Metals, Metals Park, OH, 1985).